Study of unsymmetrical dimesogens containing 4-heptylazobenzene

V. Ajay Mallia, Masahiro Funahashi and Nobuyuki Tamaoki*

Molecular Smart System Group, Nanotechnology Research Institute, National Institute of Advanced Industrial Science and Technology (AIST), Central 5, 1-1-1 Higashi, Tsukuba, Ibaraki 305-8565, Japan

ABSTRACT: 4-Heptylazobenzene (HAB) has been covalently attached to cholesterol (Ch) by varying the methylene spacers and to cyanobiphenyl (CB) moiety with an octyl methylene linkage. Enhancement of short-range translational correlations in the chiral nematic (N^*) phase has been observed by the introduction of HAB moiety. HAB–Ch dimesogens exhibit chiral smectic C (SmC^*), chiral smectic A (SmA^*) and N^* phases depending on the methylene spacer length. The dimesogen containing HAB–CB shows a SmA and an N phase. The HAB–Ch dimesogen with octyl methylene spacer shows co-existence of multiple periodicities in its SmA^* as well as in SmC^* phases. A dramatic increase of >150 nm in the N^* reflected wavelength shift ($\Delta\lambda$) with change in temperature has been observed for the HAB-Ch dimesogen containing an octyl spacer compared to the similar dimesogen that does not have a heptyl side chain. Ferroelectric switching has been studied for a representative dimesogen containing HAB-Ch having hexyl spacer in its SmC^* phase, the spontaneous polarization value was determined to be 150 nC cm^{-2} (at $125\,^\circ$C) by applying a triangular wave field. A reversible photochemical switching between SmA and N phases also has been reported for the dimesogen containing HAB–CB. Copyright © 2007 John Wiley & Sons, Ltd.

KEYWORDS: photoactive chiral dimesogens; smecic cybotactics; reflection wavelength; light driven phase transitions

INTRODUCTION

Development of novel organic photoresponsive materials has been an area of immense interest mainly due to their wide application prospects in photonics.[1] Liquid crystals (LCs) are promising materials for photonic applications since microscopic molecular perturbations occurring within them can amplify to macroscopic levels, resulting in significant changes in their optical properties.[2–6] Recently dimesogens/twins (LCs containing two mesogenic units linked through a flexible spacer) are attracting attention because they exhibit new LC phases and show properties applicable for optical materials,[6–8] information storage devices[9–11] and also as suitable dopant in glass forming LCs.[12–14] Chiral nematic (N^*) LCs possess an inherent property of selective reflection of light due to their unique helical superstructure. The wavelength of light reflected by such materials is highly sensitive to external stimuli such as temperature, pressure and impurities. These aspects have been the subjects of innumerable reports[11,15–24] and also make N^* LCs useful

in a variety of display applications. Recent study has shown that the photoinduced changes in the wavelength of the reflected light can be attributed to changes in the short-range translational correlations in some cholesterol (Ch) based LCs.[25,26] X-ray diffraction (XRD) analyses provided evidence for the changes in the size and amount of these smectic domains that result in variations of the N^* LC helical pitch. Studies have also shown that molecules which can act as smectic inducers influence the short-range translational orders in the LC phase.[25] Smectic inducers can be defined as rod-shaped moieties linked to a flexible alkyl chain. Recently it has been reported on the alteration of the range of reflected wavelength upon doping the rod-shaped molecules in N^* LC materials.[25]

In this paper we hypothesize that upon synthesizing a dimesogen in which smectic inducer is covalently attached to a chiral nematogen, short-range correlations in the nematic LC phase will enhance. N^* reflected wavelength of such LCs will be highly sensitive to the external perturbations. This will be a good method to increase the range of selective reflection in N^* LCs and to design materials for display applications. To test this hypothesis we have synthesized photoactive 4-heptylazobenzene (HAB) linked to Ch by varying the methylene chain (**7n6**, **7n8**, **7n10** and **7n12**). By covalent linking of a smectic inducer (in the present case HAB),

Correspondence to: Dr N. Tamaoki, Molecular Smart System Group, Nanotechnology Research Institute, National Institute of Advanced Industrial Science and Technology (AIST), Central 5, 1-1-1 Higashi, Tsukuba, Ibaraki 305-8565, Japan.
E-mail: n.tamaoki@aist.go.jp

microscopic translational ordering in the N* phase can increase which can in turn increase the pitch of the helix. The reason behind the synthesis of only even number of methylene linkers is because our earlier results on dimeric LCs show that even number of methylene linkers exhibits high sensitivity towards the reflected wavelength compare to their odd counter parts.[26]

To study the effect on the microscopic translational ordering in a nematic LC HAB linked to the cyanobiphenyl (CB) group (**7n8CN**) also has been prepared (Chart 1). Literature shows that there are detailed investigations of the role of terminal chain, with respect to the spacer, on the LC dimers to form smectic phases.[27,28] Present study shows the effect of translational short-range correlations on the LC properties as well as on N* reflection wavelength. LC properties of these dimesogens have been systematically studied. Electro-optical studies of a representative ferroelectric dimesogen **7n6** have also been discussed. Photoinduced *cis/trans* isomerisation of the azobenzene chromophore in **7n8CN** could be utilized to bring about an isothermal phase transition from the smectic to the nematic phases.

n =6, **7n6**; n =8, **7n8**; n=10, **7n10**; n=12, **7n12**

7n8CN
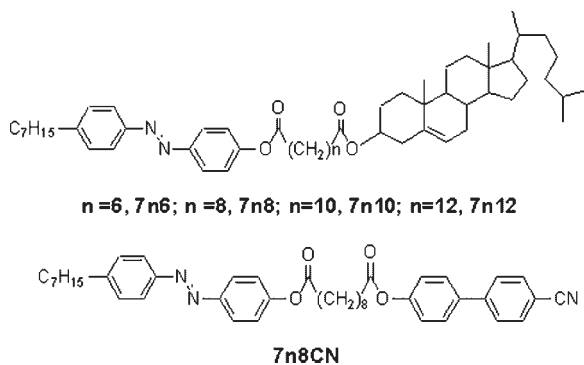
Chart 1. Investigated dimesogens

RESULTS AND DISCUSSION

Mesomorphic properties

Mesomorphic properties of the dimesogens were investigated using Polarizing Optical Microscopy (POM), Differential Scanning Calorimetry (DSC) and XRD. Dimesogen **7n6** melts to a chiral smectic C (SmC*) phase at 125.6 °C and to a N* at 149.8 °C before changing to an isotropic phase at 176.4 °C. The SmC* phase has been identified by its characteristic broken fan texture with dichiralization line and reflecting nature, observed using POM. Dimesogens **7n8**, **7n10** and **7n12** exhibit SmC*, chiral smectic A (SmA)* and N* phases in the heating and cooling cycles. In this series it can be seen that decreasing the methylene spacer between HAB and Ch unit from 12 to 6 stabilizes SmC* phase. Dimesogen containing HAB linked to CB through an octyl methylene spacer (**7n8CN**)

Table 1. Phase transition temperatures and enthalpies of dimesogens

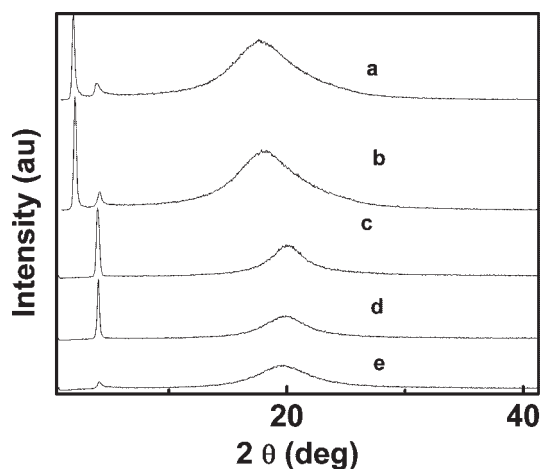|	Phase transition temperature/°C[a,b] (ΔH/kJ mol^{-1})	
	Heating	Cooling
7n6	Cr 125.6(21.0) SmC* 149.8 N* 176.4(3.8) Iso	Iso 169.9(3.4) N* 147.4 SmC* 77.3(19.7) Cr
7n8	Cr 86.4(25.6) SmC* 110.6(0.5) SmA* 126.2(0.1) N* 159.3(4.0) Iso	Iso 155.0(4.3) N* 125.2(0.1) SmA* 106.4 (0.5) SmC* 66.6(22.5) Cr
7n10	Cr 94.9 SmC* 97.4 SmA* 138.3(0.2) N* 154.1(4.7) Iso	Iso 148.1(4.2) N* 137.4(0.2) SmA* 93.6 SmC* 63.8(29.0) Cr
7n12	Cr 87.7 SmC* 90.1 SmA* 134.0(0.2) N* 146.0(4.5) Iso	Iso 145.2(3.9) N* 132.6(0.2) SmA* 86.7 SmC* 63.6(25.6) Cr
7n8CN	Cr 124.3(30.9) SmA 146.6(0.6) N 173.4(5.6) Iso	Iso 169.9(5.1) N 143.3(0.6) SmA 90.1(30.1) Cr

[a] Transition temperatures are obtained from DSC analysis at a rate of 5 °C min^{-1} in the first heating and cooling cycles.
[b] Cr, crystalline; SmC*, chiral smectic C; SmA*/SmA, smectic A; N*, chiral nematic; Iso, isotropic.
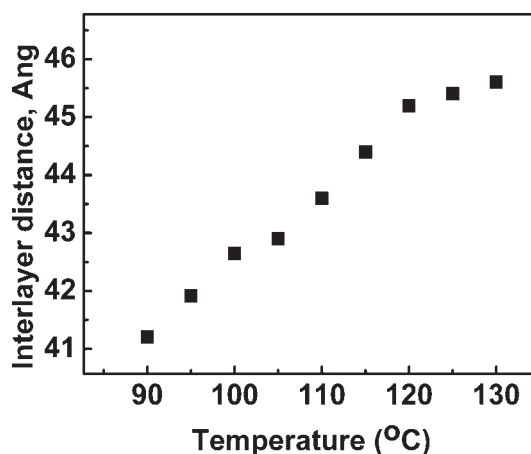
exhibits SmA and N LC phases. Phase transition temperature as well as enthalpy changes obtained for these dimesogens are summarized in Table 1.

For further characterisation of the smectic LC phases XRD studies have been carried out for the representative dimesogens **7n6**, **7n8** and **7n8CN**. Figure 1(a) and (b) shows the intensity *versus* diffraction angle profile extracted from the XRD pattern for **7n6** at 130 and 100 °C, respectively. Two peaks (θ_1 and θ_2) were seen at low angles and a weak diffuse peak was observed at wider angles. A sharp lower angle peak accompanied by a diffuse peak at higher angles is characteristic of a smectic phase in which molecules are stacked into layers with short range, liquid like positional order within the layers. The molecular length (L) of **7n6** determined from molecular model in the extended conformation using the MM2 (molecular mechanics 2) method was found to be 47.6 Å. The interlayer spacing (d) obtained from X-ray diffractogram for θ_1 at 100 °C is 42.6 Å, which is much smaller than the molecular length [Fig. 1(b)]. The momentum transfer vector, q_1 at 100 °C equals 0.15 Å. Here 'q' is defined as $q = 4\pi \sin \theta/\lambda$, which is $2\pi n/d$, where 'θ' is diffraction angle, 'λ' is wavelength = 1.54 Å, 'n' is an integer and 'd' lattice distance. At 100 °C, the interlayer spacing obtained from XRD diffractogram for θ_2 is 21.3 Å ($q_2 = 0.30$ Å). Ratio of θ_1 and θ_2 is found to be almost 2 at all temperatures and also the relative intensities of the q_1 and q_2 were not affected upon temperature change suggesting that the latter could be the second harmonic of the fundamental θ_1.

The smaller d spacing values in conjunction with striped focal conic textures and also reflecting nature confirm SmC* phase. Also, as observed for the reported SmC* phases[29] layer spacing at lower temperature was found to be decreased due to the increase in the tilt angle (Fig. 2). For **7n6** the layer spacings decreased from 45.4 Å ($q = 0.138$ Å) to 41.2 Å ($q = 0.152$ Å) on lowering the temperature.

Figure 2. Dependence of the interlayer distance observed in SmC* phase of **7n6** with temperature in the cooling cycle

Figure 3 shows the intensity profiles obtained for **7n8** at different smectic temperatures. From the figure it can be seen that all smectic phases exhibited Bragg diffraction peaks in the small-angle region, corresponding to the layer reflections, and diffuse peaks in the wide angle region, corresponding to short spacings or interchain distances. Significant point to be noticed in the XRD pattern of **7n8** is the presence of two short angle reflections (θ_1 and θ_2) and difference in the ratios of the θ_1 and θ_2 upon decrease in the temperature. In the SmA* phase [Fig. 3(e)] interlayer distances (d) calculated for θ_1 and θ_2 are 23.6 Å ($q_1 = 0.266$ Å) and 46.6 Å ($q_1 = 0.135$ Å). The d/L values obtained for θ_1 and for θ_2 are 0.91 and 0.46, respectively, which can be assigned to monolayer and intercallated arrangements.[30] In SmC* phase the intercalated distance for θ_1 decreased on lowering the temperature indicating the increase in the SmC* tilt angle. Surprisingly in SmC* phase interlayer spacing (d) corresponding to the second lower angle peak θ_2 is observed at 23.6 Å as in SmA* and does not change
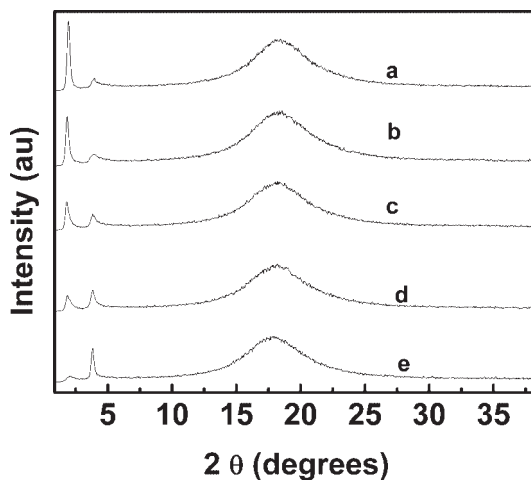

Figure 1. X-ray diffractograms of **7n6** at (a) 130 °C, SmC*, (b)100 °C, SmC*, and **7n8CN** at (c) 130 °C, SmA, (d)110 °C, SmA, (e)150 °C, N

Figure 3. X-ray diffractograms of **7n8** at (a) 85 °C, SmC*, (b)95 °C, SmC*, (c) 105 °C, SmC*, (d)110 °C, SmA*, (e)125 °C, SmA*

depending on temperature. It can be speculated that in SmC* phase short-range SmA* intercalated ordering co-exists with the monolayer tilted arrangement. Another important point to note from the XRD diffractogram of both of SmA* and SmC* phases is the ratio of θ_1 against θ_2 which decreased upon heating. At the phase transition temperature [110 °C, Fig. 3(d)] from SmC* to SmA* intensities at θ_1 and θ_2 become the same. In SmC* phase also monolayer arrangement (tilted) was found to be favourable [Figure 3(a–c)].

The dimesogen **7n8CN** exhibits only a sharp peak at lower angle at a layer distance of 21.8 Å [Figure 1(c–d)] in the SmA phase. The d/L value was found to be 0.50 confirming the formation of intercalated SmA phase. Even at the lower temperature, no peak suggesting the monolayer molecular arrangement was observed for **7n8CN**.

## Effect of temperature on reflection wavelength

The molecular ordering of N* LCs in a helical arrangement induces reflection at the wavelength satisfying the equation $\lambda_{max} = pn$, where λ_{max} is the reflection maximum, p is the pitch of the helix and n is the refractive index. Pitch length of a N* LC can increase or decrease with temperature depending on the sign of the thermal coefficient α, which equals $1/p \, [dp/dT]$, where T is the temperature. When $[dp/dT] > 0$, pitch length will increase with increasing temperature and vice versa. In the present study it has been found that $[dp/dT] < 0$. Dimesogen **7n8** exhibits a reflection band at 515 nm at 115 °C, and the reflection band red-shifted to 896 nm upon cooling to 132 °C (Fig. 4). Change in the reflection wavelength ($\Delta\lambda$) was found to be 381 nm.

We have earlier reported[26] on a change of 225 nm in the reflection wavelength ($\Delta\lambda$) with temperature for azobenzene linked to Ch with 8 methylene spacers (**n8**). The
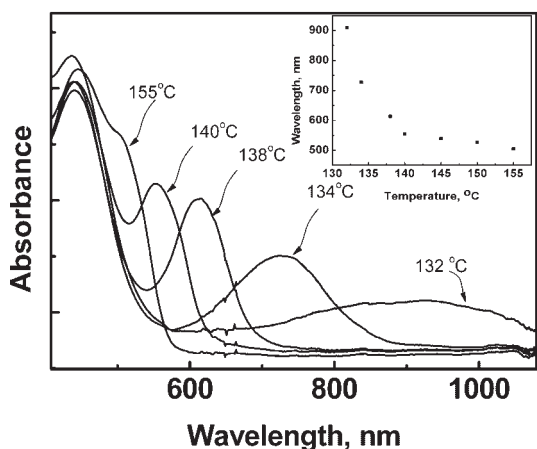
Figure 4. Absorbance spectra of **7n8** at different temperatures. Inset shows the selective reflection wavelength of the N* phases plotted as a function of temperature
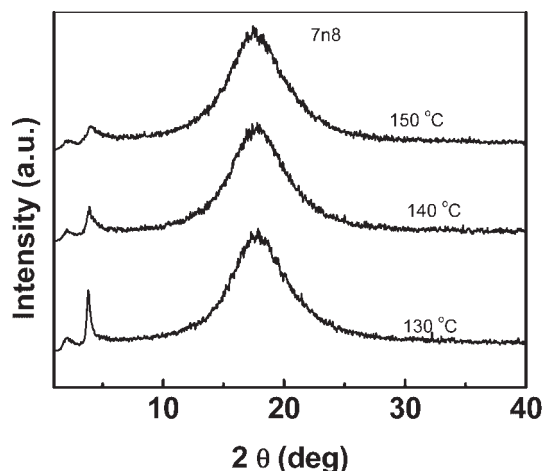
**Figure 5.** X-ray diffraction pattern of **7n8** in the chiral nematic phase

only difference between **n8** and **7n8** is the presence of a heptyl spacer at the *para* position of azobenzene. Dramatic increase of >150 nm in $\Delta\lambda$ observed in **7n8** compared to **n8** could be explained considering enhancement of the short-range translational correlations in the N* phase due to the smectic inducing effect of the dialkylazobenzene group. To explore the mechanism of shift in reflection wavelength in **7n8**, XRD studies were carried out at different temperatures. Figure 5 shows the X-ray diffractograms obtained for **7n8** at different temperatures in the N* phase (cooling cycle). X-ray diffractogram of **7n8** in the N* phase shows low intensity reflections (short-range translational correlations or smectic fluctuations) at small angles. As N* phase is cooled, the smectic fluctuations become more pronounced leading to sharpening of the small-angle peak. This is clear from Fig. 4 inset, on lowering the temperature a drastic red-shift in the wavelength was observed. These studies suggest that the mechanism of change in reflection wavelength in the dimesogen **7n8** could be due to the variation in low-range smectic correlations present in the N* phase.

In the case of dimesogens, **7n10** and **7n12** exhibit changes in reflection wavelength from 523 nm (150 °C) to 713 nm (136 °C); $\Delta\lambda = 193$ nm and 520 nm (140 °C) to 603 nm (132 °C); $\Delta\lambda = 83$ nm, respectively. On comparison of the $\Delta\lambda$ values of the azobenzene-cholesteryl dimesogens which do not have alkyl chains in the *para* position, the change in the reflection wavelength appears smaller. This could be explained by the increasing methylene spacer stabilizing the smectic phase which narrows the N* range.

Electro-optical measurements

The tilted smectic LC phases in materials composed of chiral molecules exhibit spontaneous polarization. In SmC* phase the direction of polarization is coupled to the
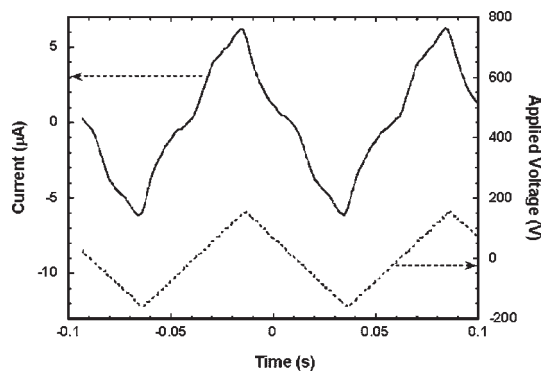
Figure 6. Oscilloscope traces of the sample current response and the applied triangular field of **7n6** at 125 °C, 10 Hz

direction of the tilt (azimuthal angle) of the molecules. By reversing the sign of an applied electric field, the molecules can be made to switch between two bistable tilting directions, resulting in an electro-optical effect. The electro-optical response was measured for a representative dimesogen **7n6** in the SmC* phase. Samples were sandwiched between two indium tin oxide (ITO) coated glass plates. Figure 6 shows the electrical response of a 9 μm cell containing **7n6** in the SmC* phase under a triangular wave voltage. The frequency was 10 Hz and the amplitude ±100 V. Because of the large viscosity and large ionic current, polarization inversion current peak is small and broadened in addition to unclear discontinuity at voltage inversion points. However, one current peak based on the polarization inversion is recorded during a half period suggesting ferroelectric behaviour. The combined area under the two peaks is a direct measure of spontaneous polarization (P_s). The polarization value was determined to be 150 nC cm^{-2} (at 125 °C). The value of P_s was comparable to the earlier reported dimeric LCs.[29]

Light driven phase transitions

Phase transition can be triggered by photochemical reactions of the LC matrices.[2,31] In LC containing azobenzene derivatives, the rod like shape of the *trans* form of azobenzenes tends to stabilize the LC phase while the *cis* form tends to destabilize it.[4,31,32] Thus, *trans–cis* photoisomerization of the azobenzene derivatives can lead to a lowering of the LC to isotropic phase transition temperature of the mixture. Recently we reported interesting photoinduced phase transitions observed in the chiral dimesogenic materials.[26,33,34] Here we describe on the SmA to N light driven phase transition observed in **7n8CN**.

Thin layers of dimesogen **7n8CN** was sandwiched between cover slips containing 5 μm glass spacers and the film was heated to the isotropic state and slowly cooled to 130 °C. At this temperature the film showed the focal conic fan shaped texture characteristic of SmA phase [Fig. 7(a)]. The film turned nematic on irradiation with light from a 500 W high-pressure mercury lamp, for 30 s filtered through a 366 nm filter, which was confirmed by the presence of nematic schlieren texture as shown in Fig. 7(b). Photolysis of *trans*-**7n8CN** would lead to partial isomerization to its *cis* form. On keeping the irradiated film of **7n8CN** at the same temperature (130 °C), *cis* to *trans* reversal of dimesogen **7n8CN** occurred, which changed the N phase to SmA [Figure 7(c)]. Thermal reversal was observed to be fast which could be due to the higher temperature and also less amount of *cis* isomer required for the phase transition.

EXPERIMENTAL

Measurements

The high-resolution proton NMR spectra of all the intermediates and the final compounds have been recorded in a Varian (300 MHz) spectrometer using the CDCl$_3$ as the solvent. The optical textures of the mesophases were observed and identified using the polarizing optical microscope (Olympus BX 60) equipped with the hot stage (Mettler, FP82 or FP 90). Electronic and reflection spectra were recorded on UV–Vis spectrophotometers (Hewlett-Packard 8453 and Otsuka Electronics MCPD-1000, respectively). The phases obtained under polarizing microscope were also confirmed using differential scanning calorimeter (Seiko
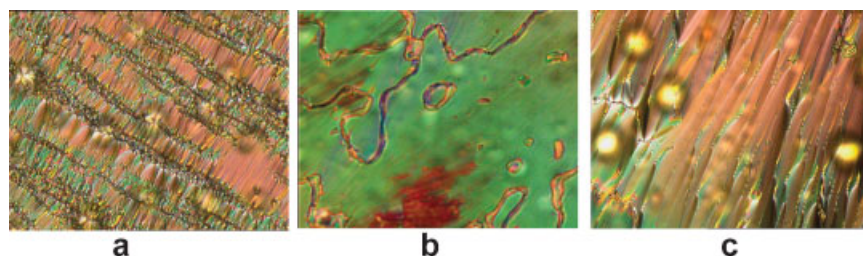
Figure 7. Optical photographs of **7n8CN** at 130 °C, in the cooling cycle (a) before photolysis SmA phase, (b) after photolysis for 30 s using 366 nm light, N phase, and (c) SmA phase regenerated after thermal *cis–trans* reversal

instrument DSC 5200). XRD patterns were obtained using a Rigaku diffractometer (Type 4037) with type graded d-space elliptical side-by-side multilayer optics, monochromated Cu Kα (40 Kv, 30 mA) and imaging plate (R-axis IV). The samples were put in quartz capillary tubes (1.5 mm diameter, 0.01 mm wall thickness) and positioned on a hot stage. The samples were heated to their isotropic state, subsequently cooled to the mesophases and then exposed to a radiation beam for 30 s with a 150 mm camera length. The N* LC samples of the dimesogens were prepared by sandwiching the uniform mixture between two glass plates with temperature control using a hot stage (Mettler, FP 82 or FP 90). A high-pressure mercury lamp (Ushio, 500 W) with suitable glass filters (for irradiation at 366 nm, Toshiba Glass Co., UV-35 + UVD-36C) was utilized as the irradiating source. Polarization switching of the dimesogenic compounds was studied using ITO electro-optical cells (9 μm, 0.16 cm^2). The sample was subjected to a triangular wave profile through a function generator (WF 1943 A, NF corporation, Japan) and a high voltage amplifier (HSA 4051, NF corporation, Japan), The sample response current was measured as a voltage generated across a 10 kΩ detection resistor connected in series with the sample. The profiles were acquired using a digital oscilloscope (TDS 3012B, Tektronix, Inc.) and transferred to a PC for further analysis. During the measurements the sample cells were placed on a hot stage (Mettler, FP 82 or FP 90).

Materials

The dimesogens investigated in the present study were prepared as described in the synthesis of related compounds.[26,33,34] These compounds were characterized based on the analytical and spectral data as illustrated below:

7n6: ^{1}H-NMR (CDCl$_3$, 300 MHz): δ 0.67–2.20 (m), 2.58 (2H, t), 2.69 (2H, t), 4.65 (1H, m), 5.39 (1H, m), 7.22 (2H, d), 7.31 (2H, d), 7.82 (2H, d), 7.93 (2H, d); Anal. Calcd for C$_{54}$H$_{80}$N$_2$O$_4$: C, 78.98; H, 9.82; N, 3.41. Found C, 78.49; H, 9.68; N, 3.30.

7n8: ^{1}H-NMR (CDCl$_3$, 300 MHz): δ 0.66–2.20 (m), 2.58 (2H, t), 2.70 (2H, t), 4.63 (1H, m), 5.37 (1H, m), 7.22 (2H, d), 7.31 (2H, d), 7.81 (2H, d), 7.92 (2H, d); Anal. Calcd for C$_{56}$H$_{84}$N$_2$O$_4$: C, 79.20; H, 9.97; N, 3.30. Found C, 78.69; H, 9.79; N, 3.18.

7n10: ^{1}H-NMR (CDCl$_3$, 300 MHz): δ 0.67–2.20 (m), 2.58 (2H, t), 2.70 (2H, t), 4.62 (1H, m), 5.37 (1H, m), 7.22 (2H, d), 7.30 (2H, d), 7.80 (2H, d), 7.93 (2H, d); Anal. Calcd for C$_{58}$H$_{88}$N$_2$O$_4$: C, 79.40; H, 10.11; N, 3.19. Found C, 79.43; H, 10.12; N, 3.04.

7n12: ^{1}H-NMR (CDCl$_3$, 300 MHz): δ 0.67–2.20 (m), 2.58 (2H, t), 2.70 (2H, t), 4.62 (1H, m), 5.37 (1H, m), 7.22 (2H, d), 7.30 (2H, d), 7.79 (2H, d), 7.90 (2H, d); Anal.

Calcd for C$_{60}$H$_{92}$N$_2$O$_4$: C, 79.60; H, 10.24; N, 3.09. Found C, 79.33; H, 10.12; N, 3.05.

7n8CN: ^{1}H-NMR (CDCl$_3$, 300 MHz): δ 0.96 (3H, t), 1.29–1.79 (22H, alkyl), 2.59 (4H, t), 2.68 (2H, t), 7.19 (2H, d), 7.31 (2H, d), 7.42 (2H, d), 7.58 (2H, d), 7.64 (2H, d), 7.70 (2H, d) 7.82 (2H, d), 7.92 (2H, d); Anal. Calcd for C$_{42}$H$_{47}$N$_3$O$_4$: C, 76.68; H, 7.20; N, 6.39. Found C, 76.56; H, 7.19; N, 6.32.

REFERENCES

1. *Molecular Switches*, Feringa BL (ed). Wiley-VCH: Weinheim, 2001.
2. Ichimura K. *Chem. Rev.* 2000; **100**: 1847–1873.
3. Ikeda T, Sasaki T, Ichimura K. *Nature* 1993; **361**: 428–430.
4. Ikeda T, Kanazawa A. *Bull. Chem. Soc. Jpn.* 2000; **73**: 1715–1733.
5. Lansac Y, Glaser MA, Clark NA, Lavrentovich OD. *Nature* 1999; **398**: 54–57.
6. Mallia VA, Tamaoki N. *Chem. Soc. Rev.* 2004; **33**: 76–84.
7. Imrie CT, Henderson PA. *Curr. Oppin. Colloid. In.* 2002; **7**: 298–311.
8. Imrie CT, Luckhurst GR. In *Hand Book of Liquid Crystals*, vol. **2B**, Demus D, Goodby J, Gray GW, Spiess H-W, Vill V (eds). Wiley-VCH: Weinheim, 1998; 801.
9. Tamaoki N, Parfenov AV, Masaki A, Matsuda H. *Adv. Mater.* 1997; **9**: 1102–1104.
10. Tamaoki N, Moriyama M, Matsuda H. *Angew. Chem. Int. Ed. Engl.* 2000; **39**: 509–511.
11. Tamaoki N. *Adv. Mater.* 2001; **13**: 1135–1147.
12. Akiyama H, Mallia VA, Tamaoki N. *Adv. Funct. Mater.* 2006; **16**: 477–484.
13. Davis R, Mallia VA, Das S, Tamaoki N. *Adv. Funct. Mater.* 2004; **14**: 743–748.
14. Tamaoki N, Aoki Y, Moriyama M, Kidowaki M. *Chem. Mater.* 2003; **15**: 719–726.
15. Feringa BL, vanDelden RA, Koumura N, Geertsema EM. *Chem. Rev.* 2000; **100**: 1789–1816.
16. Sackmann E. *J. Am. Chem. Soc.* 1971; **93**: 7088–7090.
17. Ruslim C, Ichimura K. *J. Phys. Chem. B.* 2000; **104**: 6529–6535.
18. Moriyama M, Song S, Matsuda H, Tamaoki N. *J. Mater. Chem.* 2001; **11**: 1003–1010.
19. George M, Mallia VA, Antharjanam PKS, Saminathan M, Das S. *Mol. Cryst. Liq. Cryst.* 2000; **350**: 125.
20. Lee H-K, Doi K, Hirada H, Tsutsumi O, Kanazawa A, Shiono T, Ikeda T. *J. Phys. Chem. B.* 2000; **104**: 7023–7028.
21. Burnham KS, Schuster GB. *J. Am. Chem. Soc.* 1999; **121**: 10245–10246.
22. Kurihara S, Nomiyama S, Nonaka T. *Chem. Mater.* 2000; **12**: 9–12.
23. van Delden RA, van Gelder MB, Huck NPM, Feringa BL. *Adv. Funct. Mater.* 2003; **13**: 319–324.
24. Bobrovsky AY, Shibaev VP. *Adv. Funct. Mater.* 2002; **12**: 367–372.
25. Kidowaki M, Moriyama M, Wada M, Tamaoki N. *J. Phys. Chem. B.* 2003; **107**: 12054–12061.
26. Mallia VA, Tamaoki N. *J. Mater. Chem.* 2003; **13**: 219–224.
27. Attard GS, Date RW, Imrie CT, Luckhurst GR, Roskilly SJ, Seddon JM, Taylor L. *Liq. Cryst.* 1994; **16**: 529–581.
28. Date RW, Imrie CT, Luckhurst GR, Seddon JM. *Liq. Cryst.* 1992; **12**: 203–238.
29. Lee J-W, Park Y, Jin J-I, Achard MF, Hardouin F. *J. Mater. Chem.* 2003; **13**: 1367–1372.
30. Lee DW, Jin J-I, Laguerre M, Achard MF, Hardouin F. *Liq. Cryst.* 2000; **27**: 145–152.
31. Ikeda T, Tsutsumi O. *Science* 1995; **268**: 1873–1875.
32. Ikeda T. *J. Mater. Chem.* 2003; **13**: 2037–2057.
33. Mallia VA, Tamaoki N. *Chem. Mater.* 2003; **15**: 3237–3239.
34. Mallia VA, Tamaoki N. *Chem. Commun.* 2004; 2538–2539.